ON THE ROLE OF INFORMATION AND UNCERTAINTY IN AUDITORY THRESHOLDS

Willy Wong and Suraya Figueiredo

Edward S. Rogers Dept. of Electrical and Computer Engineering
University of Toronto, Toronto, Ontario, Canada, M5S 3G4
`willy@eecg.utoronto.ca`

ABSTRACT

Any theory on the design of auditory displays must be predicated on a proper understanding of the temporal and spatial characteristics of audition. In this paper, we revisit a classic problem of psychoacoustics related to the time-dependent characteristics of auditory thresholds. We offer new insight to this area and suggest how the concept of information and uncertainty can help elucidate the process underlying auditory thresholds. We also compare similar results obtained in vision, results which have played a vital role in the design of visual displays.

1. INTRODUCTION

Psychophysics began historically with the study of sensory thresholds through the work of E.H. Weber in the 19th century. The threshold is a measure of the sensitivity of the sensory system to changes in the environment. Thresholds determine the variation in signal magnitude required for a human subject to register or apprehend a change in the sensory signal. In auditory intensity discrimination experiments, a subject is required to distinguish between two tones of intensity I and $I + \Delta I$. ΔI represents the change in intensity required for the subject to notice a difference in signal magnitude. The fractional change $\Delta I/I$ is often called the Weber fraction. Measurements of Weber fractions can be complicated by the effects of adaptation. Adaptation is due to prolonged exposure to a sensory signal and can introduce time-dependent changes to the value of the threshold.

Another complication arises naturally from the fact that there exist no unique way to define a sensory threshold. Figure 1 demonstrates this problem. Illustrated are three well-known methods for measuring thresholds in psychoacoustics. In the past, researchers have tacitly assumed that the three methods would yield comparable values for the thresholds. This assumption is now known to be false (e.g. for hearing see [1]; for vision, [2]; for the senses in general, [3]). A detailed explanation on the differences between the different methods can be found in [3] and [4].

2. THE "THRES-HOLY" TRINITY

Having accepted that there is no unique way of determining sensory thresholds, we now turn to ask what process lies at the heart of each type of experiment. In other words, what salient sensory features are highlighted by each of the three experimental method? In type I experiments ('gated' or 'difference'), the subject is presented a tone followed by a silent period and a second tone. The subject's task is to determine whether (1) both tones are of identical intensity I (i.e. the pedestal intensity), or (2) of differing
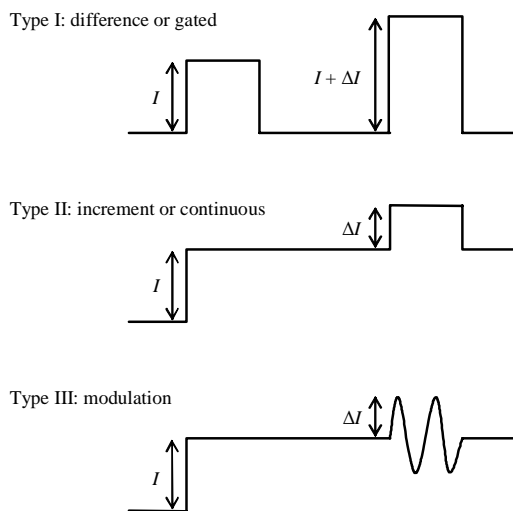

Figure 1: *Three methods for defining thresholds.*

intensities (i.e. one is I and the other is $I + \Delta I$). The threshold measured by this method is the result of imperfect memory in comparing tone 1 to tone 2. Such imperfections may arise from sensory noise or cognitive noise or both (e.g. [5]).

The type II threshold ('continuous' or 'increment') involves determining the subject's sensitivity to continuous changes in signal magnitude. The subject is presented with one of two possible choices, either (1) a constant signal with intensity I or (2) a signal with intensity I followed by an increment ΔI superimposed continuously upon the pedestal. The subject's task is to determine which of the two possibilities was heard. In contrast to the type I experiments, this approach does not involve the comparison of two tones in memory. What we shall demonstrate in this paper is that the major factor underlying intensity resolution in the case of type II or 'incremental' thresholds is the effect of adaptation.

Finally, we will address the type III measurement most commonly called 'modulation'. The method of modulation was popularised by the classic experiments of Riesz [6]. Riesz used the method of modulation to avoid artifacts that appeared because of the sharp onset of the signal. A sharp onset introduces high frequency components in the signal (e.g. Gibb's effect) and can be a source of contamination since it provides extra cues to the subject (e.g. [7]). Riesz's modulation technique involves the detection of beat frequencies produced by two pure tones differing slightly in frequency. By inspection, it is easy to conclude that the tech-

nique of modulation is closest to the type II technique. This hypothesis is further supported by the fact that the results of Riesz's experiment are similar to the results obtained from the incremental method. We shall demonstrate later that the results of Riesz follow in a straightforward manner from the same theory used to account for incremental thresholds. It also bears to note briefly that the modulation technique is similar to the method by which flicker fusion is measured in vision.

3. THEORIES OF THRESHOLDS

The modern approach to analysing data from threshold experiments is to use signal detection theory to study the effects of sensitivity (d') as a function of pedestal intensity [8]. This technique has been successful and relies on assumptions pertaining to the shape of certain underlying distributions. These distributions govern the error associated with the internal representation of sensory signals. The error may be due to sensory or cognitive noise, and the distribution is generally assumed to be Gaussian with fixed variance. Laming in particular has developed an entire sensory theory based upon the so-called concept of 'differential coupling' which leads naturally to the signal detection approach in threshold analysis [3].

Successful as it is, the signal detection approach has provided a plausible answer for only type I thresholds. It fails otherwise to provide a simple, conceptual explanation for type II and type III thresholds. Green and Swets, for example, noted that the receiver-operator characteristics (ROC) for type II thresholds deviate substantially from the prediction of a normal distribution, fixed variance model [8]. They went so far as to propose an alternative model where the underlying distributions for noise and noise plus signal remained Gaussian, but with differing values of variance for the noise only and the noise plus signal cases. Laming continued this idea by formulating the "non-central chi-squared model" which accounts for the asymmetry between the noise and the noise plus signal cases [3]. However this model, even if correct, is mathematically complex and does not readily account for the time-dependence of thresholds.

We propose a relatively simpler explanation for the results of type II and type III threshold measurements in terms of the information transmission by auditory neurons. Our theory is able to account for both the shape of the Weber fraction, its time-dependence as well as many threshold equations discovered empirically. We will now present our theory and show its consequences.

4. INFORMATION TRANSMITTED BY NEURONS

The entropy theory is a mathematical theory of the senses under development for over 30 years (e.g. [9]). The central idea to this approach is that uncertainty underlies perception, and that the task of perception is to remove or reduce this uncertainty. When uncertainty is gone, the process of perception ceases. Uncertainty is calculated at the level of the sensory receptor. We model the receptor uncertainty in terms of the mathematics of entropy (or information theory) as pioneered by Ludwig Boltzmann in physics and Claude Shannon in electrical engineering. In analogy with Boltzmann where he related mathematical entropy to measurable or thermodynamic entropy through his famous equation $S = -k_B H$, we too relate mathematical entropy to the response of the neuron through the equation

$$F = kH, \tag{1}$$

where H is uncertainty or entropy, k is a constant, and F is the neural firing rate. The remainder of this section will be devoted to deriving an expression for the uncertainty H.

In this abstract we lack the space to give a full derivation of the uncertainty function H. However, details can be easily found in any of a number of papers written on this subject (e.g. [10] [9] [11] [12]), although the reader is warned that theory has undergone continual evolution since the 1970's. The version we shall use here is the one documented in [12].

The basic premise for calculating H is to assume that the receptor samples the sensory signal to estimate the magnitude of the input. The uncertainty in signal magnitude is attributed to the variability or fluctuation in the signal at the receptor level. For example, it is well-known that fluctuations in the number of photons at the photoreceptor level follows a Poisson distribution. The receptor uncertainty is then calculated from the signal distribution using the Boltzmann-Shannon definition of information

$$H = -\int p(x) \ln p(x) \, dx. \tag{2}$$

Fluctuations in the signal magnitude can follow a non-Gaussian distribution although the sample means will be normally distributed according to the central limit theorem. The variance of the distribution will also be reduced by a factor m representing the sample size. Hence $p(x)$ in (2) will be a normal distribution with variance σ_S^2/m. The noise in the system is assumed to be uncorrelated with the input and is Gaussianly distributed. Calculating the transmitted information by taking the difference between the entropy of signal plus noise and the entropy of noise alone, we obtain

$$H = \frac{1}{2} \ln \left(1 + \frac{\sigma_S^2/m}{\sigma_N^2} \right). \tag{3}$$

H represents the receptor uncertainty in sampling the signal magnitude, σ_S^2 is the variance of the signal distribution, m the sample size and σ_N^2 is the variance of the noise.

Those readers finding it difficult to follow the derivation of (3) are invited to check past references where a full derivation has been given. Otherwise, it should be noted that (3) resembles the expression for channel capacity as derived by Shannon for a channel with Gaussian signal and noise [13].

Two additional relationships are required to develop a usable form for H. The first relates the fluctuations as observed in the receptive field with the signal magnitude I. This amounts to postulating a relationship between the mean of the signal and its variance. For example in vision, photon statistics obey a Poisson distribution where variance equals the mean. In audition, the analysis is trickier because the auditory signal undergoes a number of transformations, from fluctuations in air pressure to fluctuations in fluid, before reaching the receptive sites. However, it is plausible to assume that signals of larger magnitude will be associated with greater fluctuations. Thus the monotonic relationship between variance and mean should take the form

$$\sigma_S^2 \propto (I + \delta I)^p, \tag{4}$$

where I is the signal magnitude or mean, p is a constant that can be derived in principle from the physical considerations of the transduction process, and δI is a term that accounts for the non-zero fluctuations at the receptor level in the absence of a signal.
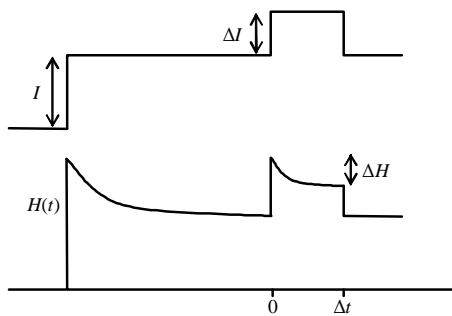
Figure 2: *Solution of Eq. (9) to the type II stimulus profile.*

Figure 3: *Visual flash thresholds measured by Roufs [18] at different pedestal intensities.*

When σ_N^2 is taken to be constant, (3) can be rewritten with (4) as

$$H = \frac{1}{2} \ln \left(1 + \frac{\beta \left(I + \delta I \right)^p}{m} \right), \qquad (5)$$

where β is a constant amalgamated from σ_N^2 and the proportionality constant in (4). The only remaining unknown quantity is the sample size m. We assume that the receptor increases its sample size over time to improve its estimate of the sample mean. If m_{eq} denotes the optimal or equilibrium sample size, then the sampling rate dm/dt will change according to the following relationship

$$\frac{dm}{dt} = f \left(m - m_{eq} \right), \qquad (6)$$

where f is some function. Assuming that m does not differ appreciably from the equilibrium value m_{eq}, we can expand (6) as a Taylor series around $m = m_{eq}$ with the restriction that dm/dt at $m = m_{eq}$ equals zero. This condition simply implies that sampling will stop when m reaches its equilibrium value. Truncating the expansion to first-order we have

$$\frac{dm}{dt} = -a \left(m - m_{eq} \right), \qquad (7)$$

where a is a positive inverse time constant. Finally, since it is expected that larger sample sizes are associated with signals of larger magnitude, we take m_{eq} to be a monotonic function of I, i.e.

$$m_{eq} = m_{eq}^0 \left(I + \delta I \right)^q, \qquad (8)$$

where q is a fixed exponent and m_{eq}^0 is a constant to assure the correct units for m_{eq}.

Summarising the three master equations, we have

$$F = kH$$
$$H = \frac{1}{2} \ln \left(1 + \frac{\beta \left(I + \delta I \right)^p}{m} \right) \qquad (9)$$
$$\frac{dm}{dt} = -a \left[m - m_{eq}^0 \left(I + \delta I \right)^q \right].$$

The solution of these three equations for any function $I = I \left(t \right)$ allows us to predict the neural response (in terms of firing frequency) as a function of both signal magnitude I and signal duration t. That is, we can solve for $F = F \left(I, t \right)$ given any time-varying stimulus $I \left(t \right)$. In several earlier papers, we demonstrated the utility of the equations in predicting a wide range of experimental
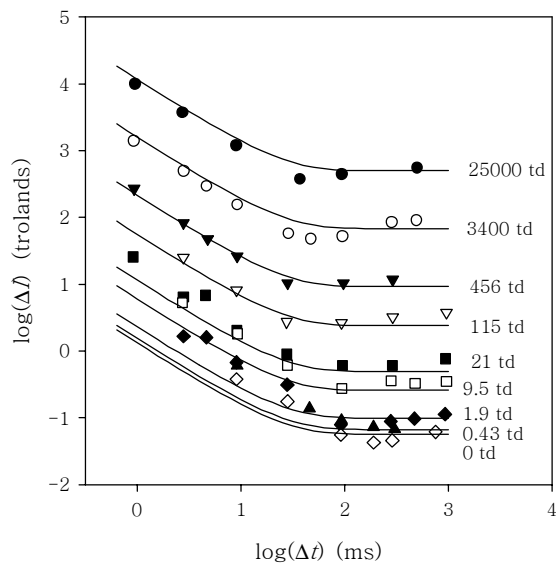
results observed at the neural level [11] [12]. Equation (9) has been used to estimate adaptation curves, spontaneous neural activity, driven firing rate curves, recovery and the response to other signal profiles with considerable success.

In the next section, we shall use these same equations with an additional threshold hypothesis to help elucidate the process underlying type II and type III thresholds.

5. THRESHOLD HYPOTHESIS AND RESULTS

We begin by solving the neural response to a type II signal profile. Figure 2 illustrates the associated neural response as a function of signal duration. Note that this result is in good qualitative agreement with the results obtained in the cat auditory nerve [14]. We now introduce the threshold hypothesis governing the detection of the increment: *an increment is detected if and only if the change in uncertainty (or the change in firing rate) over the interval of the increment exceeds a constant ΔH.* In other words, there must be a reduction in the receptor uncertainty (or firing rate) before an increment is detected. Mathematically we can state this hypothesis as

$$H \left(I + \Delta I, 0 \right) - H \left(I + \Delta I, \Delta t \right) \geq \Delta H. \qquad (10)$$

ΔH is a constant independent of the signal magnitude I. Note that our threshold hypothesis or condition is similar to Fechner's conjecture of the constant subjective jnd (just noticeable difference).

The threshold condition along with the solution of the H function to the type II signal profile will permit a numerical estimate of the Weber fraction $\Delta I/I$ as both a function of I and of Δt. However, we can do much better than that because, for relevant physiological parameters, the term $\Delta I / \left(I + \delta I \right)$ is always small. Furthermore, we have found ΔH to be small permitting us to expand the complex expression in (10) to first-order in $\Delta I / \left(I + \delta I \right)$
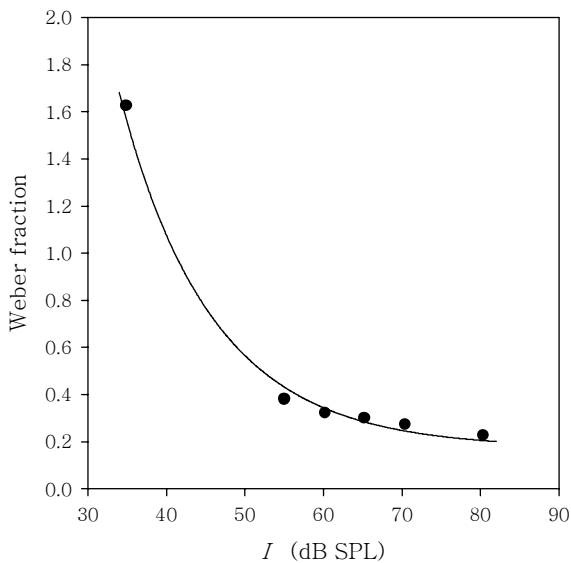
Figure 4: *Data of Carlyon and Moore [1] showing Weber fraction as a function pedestal intensity.*
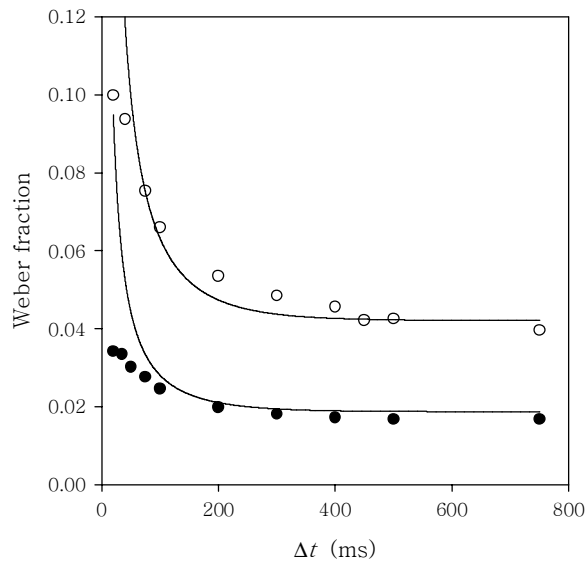

Figure 5: *Data from the classic study by Garner and Miller [7]. Weber fraction as a function of increment duration.*

and ΔH to obtain

$$\frac{\Delta I}{I} = \frac{2\Delta H}{q\left(1 - e^{-a\Delta t}\right)}\left(1 + \frac{\delta I}{I}\right)\left(1 + \frac{1}{\beta\left(I + \delta I\right)^{p-q}}\right). \tag{11}$$

These approximations will become apparent when (11) is compared with data. Equation (11) is the master equation from which many empirical threshold equations can be derived. First consider the case where δI can be ignored (i.e. $\delta I \ll I$). This will occur for most values of I above threshold. Holding Δt constant, we rewrite (11) as

$$\frac{\Delta I}{I} = A + \frac{B}{I^{p-q}}, \tag{12}$$

where A and B are constants. This is the empirical equation proposed by Riesz to account for his threshold data [6]. If we instead hold I constant and look at the Weber fraction as a function of increment duration, we find

$$\frac{\Delta I}{I} = \frac{C}{\left(1 - e^{-a\Delta t}\right)}, \tag{13}$$

where C is a constant. Equation (13) accounts nicely for many experimental results obtained from time-dependent measurements of the Weber fraction (e.g. [7]).

Returning to (11), if we look at the limit as $I \longrightarrow 0$, we have

$$\frac{\Delta I}{I} \longrightarrow \frac{D}{I}, \tag{14}$$

where D is a constant. In other words, as I approaches zero, the Weber fraction falls with slope one with respect to I. This is in agreement with observations made in connection with the loudness function [15]. When I is set equal to 0, the type II measurement becomes an experiment for *absolute thresholds*. Setting $I = 0$ in (11), we obtain

$$\Delta I = \frac{\Delta I_\infty}{1 - e^{-a\Delta t}}, \tag{15}$$

where ΔI_∞ is a constant representing the absolute minimum threshold. Equation (15) was proposed to account for the absolute threshold in audition [16] [17]. Finally, if the stimulus duration is much shorter than the inverse time constant a (i.e. $\Delta t \ll 1/a$), we can take a first-order expansion of (15) in terms of $a\Delta t$ to obtain

$$\Delta I \cdot \Delta t = E, \tag{16}$$

where E is a constant. Equation (16) is simply a statement of Bloch's law.

We have shown thus far that (11) confers certain explanatory powers by unifying many of the threshold equations that have been discovered empirically. The next step is to compare the predictions of the equation to experimental data. We begin first with vision. In the study of Roufs [18], visual flash thresholds were measured under a variety of conditions using an experimental setup identical to the intensity profile shown in Figure 2 (i.e. a type II threshold). The data from the experiment are plotted in Figure 3 showing ΔI as a function of increment duration Δt. Pedestal intensity I is set as a parameter in the experiment. The salient feature of the data is that the threshold decreases as a function of increasing increment duration. This is what is predicted by (11). While the full details of the curve-fit are not provided here (for details please see [18]), it suffices to note that a total of 7 parameters were used to fit 9 equations *or an average of less than one parameter per curve.*

Next we consider a demonstration with auditory data. In the study of Carlyon and Moore [1], they measured the threshold from a type II experiment for tones at 500 Hz. We combined this study with an older study by Garner and Miller using data obtained also at 500 Hz [7]. In total 5 parameters were used to fit 3 curves for an average of just over 1.5 parameters per curve. The data are shown in Figs. 4 and 5. Note the poor fit in Figure 5 for small Δt. This is entirely consistent with what we now know about the Garner and Miller data – that high frequency cues may have given the subjects an advantage in detecting shorter increments.
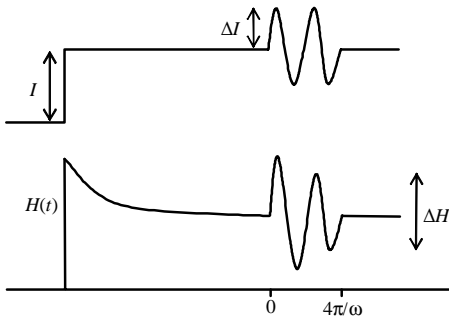
Figure 6: *Solution of Eq. (9) to the type III stimulus profile.*

Figure 7: *Flicker sensitivity as a function of modulation frequency. Data of Roufs [18].*

In passing, we note that (11) is an equation of 5 parameters. While 5 parameters may seem excessive, we must remember that (11) can handle variations in both pedestal intensity and increment duration. For example, any arbitrary mathematical expression created to fit $\Delta I/I$ vs. I data will require at least 3 parameters (c.f. Riesz's proposed equation [6]). Similarly $\Delta I/I$ vs. Δt data will require at least 2 parameters (c.f. Plomp and Bouman's proposed equation [16]). Hence, $2+3$ parameters seems to be a reasonable number of parameters for an equation that handles both intensity and duration.

A final remark regarding ΔH. Equation (11) predicts a linear relationship between the threshold (i.e. ΔI) and ΔH. Linearity here implies that a negative increment (i.e. a decrement) will obey the same equation as a positive increment. This is in fact what has been observed experimentally [18]. When an experiment is carried out with a decrement, it was found that the value of the threshold is identical to the threshold obtained for an increment, as predicted by (11).

6. SPECULATIONS AND FUTURE WORK

In this section we outline some recent work in extending our theory to type III thresholds. We begin once again by solving (9) to obtain the time-dependent neural response or uncertainty H. The theoretically predicted response to a sinusoidal input $I(t) = I + \Delta I \sin(\omega t)$ is shown in Figure 6. Note that the solution at $t > 0$ will have both a transient and (for modulation periods of sufficient length) a steady-state component. Since our primarily application will be for flicker fusion phenomena in vision (where the flicker threshold is defined for steady-state conditions), we will only calculate the threshold in the steady-state region. Let us denote the steady-state response as H_{SS}. The threshold hypothesis then states that the excursion between the highest and lowest value of the uncertainty or response function must exceed a constant ΔH:

$$H_{SS}(\pi/4\omega) - H_{SS}(3\pi/4\omega) \geq \Delta H. \quad (17)$$

Using the same approximations used in the derivation of (11), we take a first order Taylor series expansion in both $\Delta I/(I + \delta I)$ and ΔH to obtain

$$\frac{\Delta I}{I} = \Theta(\omega)\,\Delta H \left(1 + \frac{\delta I}{I}\right)\left(1 + \frac{1}{\beta(I + \delta I)^{p-q}}\right), \quad (18)$$
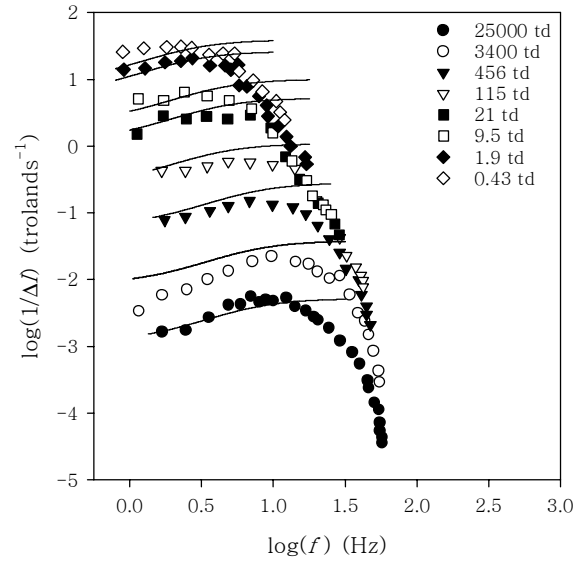
where $\Theta(\omega)$ is a function of the modulation frequency $\omega = 2\pi f$:

$$\Theta(\omega) = \sqrt{\frac{a^2 + \omega^2}{a^2(p-q)^2 + p^2\omega^2}}. \quad (19)$$

With the exception of the multiplicative factor, both (11) and (18) are identical in form. This implies that the value of the threshold for a type II experiment can be related to the value of a type III threshold by the following equation

$$\log\left(\Delta I/I|_{\text{type II}}\right) = \log\left(\Delta I/I|_{\text{type III}}\right) + G(f), \quad (20)$$

where $G(f)$ is a function of the modulation frequency but not the pedestal intensity. This relationship was observed recently in auditory experiments [19]. In the study by Wojtczak and Viemeister, they measured both the type II and the type III threshold for different pedestal conditions and obtained the following equation governing the relationship between the two thresholds,

$$\log\left(\Delta I/I|_{\text{type II}}\right) = 0.88\log\left(\Delta I/I|_{\text{type III}}\right) + \text{constant}(f). \quad (21)$$

Apart from the slope, (20) and (21) are identical. The failure of the theory to predict a slope less than one is a mystery to us, although it should be noted that certain assumptions were made in the derivation of (18) which may not match the conditions under which (21) was determined (i.e. steady vs. non–steady state thresholds).

Finally, we compare the predictions of (18) to data obtained from flicker fusion experiments. Flicker is the phenomenon whereby the visual system detects temporal fluctuations in luminance. Flicker fusion is a type III threshold experiment, and sensitivity to flicker is defined as the reciprocal of the threshold, i.e. $1/\Delta I$. The flicker threshold has played an integral role in defining a standard for televisions, movies and video display units. Flicker is most easily observed for mid-range frequencies (3-15

Hz) with sensitivity falling off rapidly for higher frequencies. This falloff has been attributed to the low-pass characteristics or "sluggishness" of the visual system. Sensitivity also decreases for the lower frequencies; currently there is no known mechanism to explain this behaviour. However we shall see shortly that the falloff at low frequencies can be explained by our theory.

In Figure 7, the flicker fusion results of Roufs [18] are shown. Thresholds were measured under steady-state conditions and thus (18) can be used to fit the data. The solid lines show the predictions of (18) *with the same parameter values used to generate the curves in Figure 7.* We see that the success of this method is mixed. On the one hand, the theory predicts the correct spacing between the different curves. More importantly, the theory also predicts the distinctive sigmoidal-like rise in sensitivity at low frequencies found in the data. However, the theory fails to show any drop in sensitivity for high modulation frequencies. This is not surprising to us – we have, thus far, made no provisions to incorporate low-pass characteristics associated with the sensory system in our theory. Recently we have sought to rectify this matter [20]. However we have yet to find an approach beyond making *ad hoc* modifications to the current theory. Part of the problem is that we do not know whether the cutoff occurs because of peripheral or central mechanisms. Presently this is one area we are actively pursuing.

7. CONCLUSIONS

In this paper we have suggested that sensory information or uncertainty is the primary process mediating threshold phenomena of the type II and type III variety. Our theory complements the role that signal detection theory has in providing a possible explanation for type I thresholds. Through the additional use of a threshold hypothesis, we were able to derive a number of well-known empirical observations and equations within psychoacoustics. It can be shown that the theory is general enough to encompass results from the other senses, particularly from vision. The salient feature of our work is the idea that threshold is achieved only when a fixed amount of information is transmitted from the neural periphery.

In closing, we make several remarks as to how a theory of thresholds can be used in the design of an auditory display. Recently, there has been an interest in using auditory displays to render entire visual scenes (e.g. [21]). The mapping of a visual scene onto an auditory display requires good understanding of the spatial and temporal characteristics of both vision and audition. While our theory at present only accounts for temporal effects, it does demonstrate that, apart from differences in parameter values, the temporal characteristics of vision are similar to that of audition. This would tend to suggest that a visual scene can, in principle, be mapped onto an auditory scene with only the changes to allow for differences in spatial and temporal resolution.

8. REFERENCES

[1] R.P. Carlyon and B.C.J. Moore, "Continuous versus gated pedestals and the 'severe departure' from Weber's law," *Journal of the Acoustical Society of America*, vol. 79, pp. 453-460, 1986.

[2] T.N. Cornsweet and H.M. Pinsker, "Luminance discrimination of brief flashes under various conditions of adaptation," *Journal of Physiology*, vol. 176, pp.294-310, 1964.

[3] D. Laming, *Sensory Analysis*, Academic Press, New York, U.S.A., 1986.

[4] N.F. Viemeister, "Psychophysical aspects of auditory intensity coding," in *Auditory Function: Neurobiological Bases of Hearing*, Wiley, New York, U.S.A., 1988, pp. 213-241.

[5] N.I. Durlach and L.D. Braida, "Intensity perception. I. Preliminary theory of intensity resolution," *Journal of the Acoustical Society of America*, vol. 46, pp. 372-383, 1969.

[6] R.R. Riesz, "Differential intensity sensitivity of the ear for pure tones," *Physical Review, Series 2*, vol. 31, pp. 867-875, 1928.

[7] W.R. Garner and G.A. Miller, "Differential sensitivity to intensity as a function of the duration of the comparison tone," *Journal of Experimental Psychology*, vol. 34, pp. 450-463, 1947.

[8] D.M. Green and J.A. Swets, *Signal Detection Theory and Psychophysics*, Krieger, New York, U.S.A., 1966.

[9] K.H. Norwich, *Information, Sensation and Perception*, Academic Press, New York, U.S.A., 1993.

[10] K.H. Norwich, "On the information received by sensory receptors," *Bulletin of Mathematical Biology*, vol. 39, pp. 453-461, 1977.

[11] K.H. Norwich and W. Wong, "A universal model of single-unit sensory receptor action," *Mathematical Biosciences*, vol. 125, pp. 83-108, 1995.

[12] W. Wong, *On the Physics of Perception*, unpublished doctoral dissertation, University of Toronto, Canada, 1997.

[13] C.E. Shannon, "A mathematical theory of communication," *Bell System Technical Journal*, vol. 27, pp. 379-423, 1948.

[14] R.L. Smith and J.J. Zwislocki, "Short-term adaptation and incremental responses of single auditory-nerve fibers," *Biological Cybernetics*, vol. 17, pp. 169-182, 1975.

[15] W.S. Hellman and R.P. Hellman, "Effect of the shape of the loudness function on the Weber fraction: Predictions and measurements," Abstract #220 in *ARO Midwinter Meeting*.

[16] R. Plomp and M.A. Bouman, "Relation between hearing threshold and duration for tone pulses," *Journal of the Acoustical Society of America*, vol. 31, pp. 749-758, 1959.

[17] J.J. Zwislocki, "Theory of temporal auditory summation," *Journal of the Acoustical Society of America*, vol. 32, pp. 1046-1060, 1960.

[18] J.A.J. Roufs, "Threshold perception of flashes in relation to flicker," in *The Perception and Application of Flashing Lights*, University of Toronto Press, Toronto, Canada, 1971.

[19] M. Wojtczak and N.F. Viemeister, "Intensity discrimination and detection of amplitude modulation," *Journal of the Acoustical Society of America*, vol. 106, pp. 1917-1924, 1999.

[20] S. Figueiredo, *Explaining Flicker Fusion Using the Entropy Theory*, unpublished undergraduate thesis, University of Toronto, Canada, 2002.

[21] P.B.L. Meijer, "An experimental system for auditory image representations," *IEEE Transactions on Biomedical Engineering*, vol. 39, pp. 112-121, 1992.